UJEAS

UNIZIK JOURNAL OF ENGINEERING AND APPLIED SCIENCES

UNIZIK Journal of Engineering and Applied Sciences 6(3), September (2026), 3611-3623
Journal homepage: https://journals.unizik.edu.ng/index.php/ujeas
PRINT ISSN: 2992-4383 || ONLINE ISSN: 2992-4391

Reconfigurable Intelligent Surface Assisted Covert Communication for Smart Grid Systems

Sandra. C. Nwokoye*
Electronic and Computer Engineering, Nnamdi Azikiwe University, Awka, Anambra State
Gerald. C. Nwalozie
Electronic and Computer Engineering, Nnamdi Azikiwe University, Awka, Anambra State
Stephen. U. Ufoaroh
Electronic and Computer Engineering, Nnamdi Azikiwe University, Awka, Anambra State,
Christiana. C. Okezie
Electronic and Computer Engineering, Nnamdi Azikiwe University, Awka, Anambra State

Corresponding Author's E-mail: sc.nwokoye@unizik.edu.ng

Abstract
In this paper, we consider a reconfigurable intelligent surface (RIS)-assisted covert communication for enhancing the security of the smart grid system. Specifically, we exploit the reconfigurability potentials of the RIS and develop an intelligent covert communication system to enhance the security of the communication within the advanced metering infrastructure (AMI) of the smart grid system. The design objective is to maximize the covert rate at the smart meters while satisfying the maximum transmit power constraint of the transmitter, the constant modulus constraints of the RIS, and to minimize the probability of the monitor/attacker detecting the transmitter's transmission behavior, thus ensuring the secure transmission of private information. We adopt some convex approximation techniques to reformulate the resulting problem into a relaxed convex optimization problem. We proposed a low-complexity and sub-optimal solution based on the alternating optimization approach. Simulation results are provided showing the effectiveness of the proposed intelligent covert communication system as compared to the other baseline schemes.
Keywords: Reconfigurable intelligent surface, covert communication, smart grid, advanced metering infrastructure, smart meters.

1. Introduction

The rapid evolution of smart grid technology has transformed the way electricity is generated, transmitted, and consumed. This has significantly improved efficiency, reliability, and sustainability in modern energy systems. This performance improvement is primarily due to the integration of Information and Communication Technology (ICT), the Internet of Things (IoT), and Artificial Intelligence (AI) into power networks, enhancing the generation, transmission, distribution, and utilization of electricity. Despite the promising advancements, the widespread adoption of smart grids faces challenges such as cybersecurity risks, technological integration issues, and data management complexities. As a result, providing adequate and efficient security schemes for smart systems has recently received a lot of attention. The term Smart Grid (SG) refers to advanced power network that integrates communication, automation, and energy management technologies to enhance efficiency, reliability, and sustainability. The SG architecture consists of the following layers: Power Generation and Transmission Layer, the transmission network, the Communication and Control Layer, and the Distribution and End-User Layer (Agung & Handayani, 2022) as shown in figure. 1. As a result, both physical and cybersecurity challenges are present throughout the entire SG network, spanning from the generation system to the distribution system and the cloud space.

The Advanced Metering Infrastructure (AMI) is at the heart of the information metering and measurement of the SG system. It is the AMI that is responsible for the bi-directional communication of loads and user consumption data between utility companies and energy consumers. This action helps in the implementation of control signals and commands that are needed in taking necessary control actions, as well as in Demand Side Management (DSM). The AMI includes smart meters, communication networks, and data management systems, as well as a means of collecting data into software applications and interfaces (Onoshakpor & Okafor, 2017). Therefore, due to the sensitive nature of the actions carried out by the AMI for the optimum realization of the SG's performance and maintenance of the integrity of the SG system, the AMI is constantly vulnerable to attacks and exploitation.

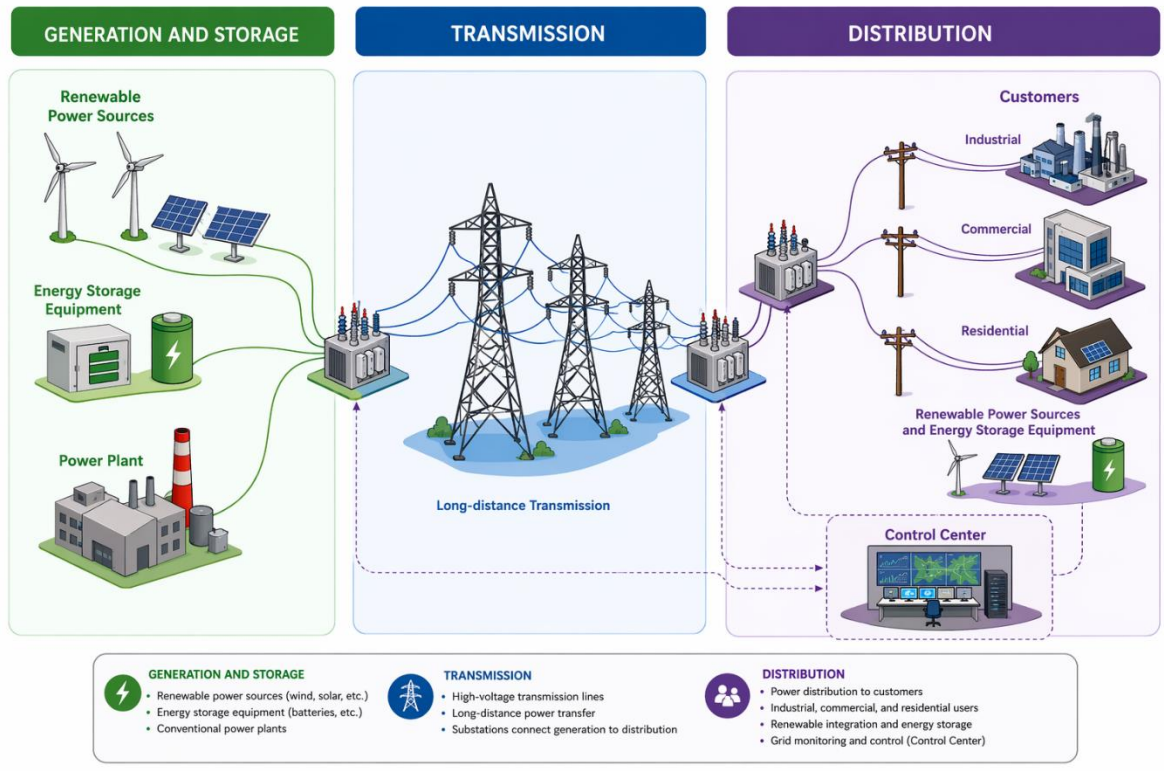


Figure 1: architecture of a Smart Grid System.

There have been recent efforts at developing and implementing solutions in the literature with regard to securing the SG system. These recent efforts include SG security survey in (Lieskovan et al., 2019), protecting the SG from cyber-attacks in (Bishowjit, 2024), and advanced metering infrastructure protection in (Rohokale & Prasad, 2016). Equally, the authors in (Onoshakpor & Okafor, 2017) proposed a Smart Grid Convoluted Network (SGCN) intending to avert any possible cyber-attacks that will affect the computational requirements of SG applications. Regrettably, the security of SG supporting core infrastructures is still compromised. These infrastructures include the remote monitoring and control system, known as the Supervisory Control and Data Acquisition (SCADA) system, Energy Management System (EMS), power system communication infrastructure, and the computational and storage resources (Upadhyay & Sampalli, 2020). Therefore, there is a great need to adequately secure and monitor these infrastructures to avoid the manipulation of their vulnerabilities to attack the SG system, which can lead to a disaster in the SG system. The use of covert communication is seen as a potential solution to enhance security and privacy for future wireless networks, as it can allow monitors to detect with a low probability the transmitter's transmission process. As a result, a secure transmission of private information can be ensured. A Covert Communications Network (CCN) is a connected, overlay, Peer-to-Peer (P2P) network being used to support communications within a group in which the survival of the group depends on confidentiality and anonymity for communications, concealment of participation in the network to both other members of the group and external eavesdroppers, and resilience against disconnection (Bash et al., 2015).

Reconfigurable Intelligent Surface (RIS), also known as Intelligent Reflecting Surface (IRS), has gained significant attention recently, as a low-cost and compact transformational technology for future wireless systems (Nwalozie & Haardt, 2023b; Wu et al., 2021; Wu & Zhang, 2020). An RIS is a planar surface composed of a large number of passive reflecting elements that are closely packed together and a smart controller. Each of the reflecting elements is capable of controlling the phase and/or amplitude of the incident waveform independently (Gong et al., 2020). By strategically deploying RISs in wireless networks and intelligently coordinating their reflections, it is possible to flexibly reconfigure the signal propagation and/or the wireless channels between the transmitters and the receivers to achieve desired realizations or distributions, e.g., the reflected signals can add constructively at the intended users and/or destructively at the unintended users (Wu et al., 2021). Thus, signal processing using RISs represents a unique approach to fundamentally tackle the problem of wireless channel fading impairment and interference, which could potentially result in a quantum leap improvement in wireless communication capacity and reliability. Due to these potentials, RIS-aided communication systems have received significant attention in the last few years, where various RIS-aided communication systems have been studied, such as millimeter-wave (mmWave) communications (Ardah et al., 2021; Gherekhloo et al., 2024), cognitive radio (Yuan et al., 2021), Dynamic Time Division Duplexing (DTDD) system (Nwalozie et al., 2022; Nwalozie & Haardt, 2023a), and Unmanned Aerial Vehicle (UAV) communications (Pogaku et al., 2022).

Motivated by the inherent benefits of the RIS and the need to design and implement reliable, secure, and intelligent solutions to enhance the security of SG systems, this work exploits the advantages offered by covert communication along with the potential benefits of the RIS to enhance the security of SG systems. To the best of the author's knowledge, there has been no work so far considering the integration of both techniques in the literature for the enhancement of the security of the SG system. We consider the problem of maximizing the covert rate at the smart meters while satisfying the maximum transmit power constraint of the transmitter, the constant modulus constraints of the RIS, and minimizing the probability of the monitor/attacker detecting the transmitter's transmission behavior, thus ensuring the secure transmission of private information. The formulated optimization problem is non-convex and hard to solve due to the coupling between the optimization variables and some of the non-convex constraints. Then, to obtain a low-complexity, suboptimal solution, we adopt the alternating optimization (AO) approach to update the active transmit beamforming vector and the passive RIS reflection vector sequentially. AO is adopted to decouple the original coupled nonconvex problem into a sequence of tractable subproblems. This will limit the search space and also lower the complexity involve in finding the optimal solution. We adopt some convex approximation techniques (semidefinite relaxation (SDR)) to recast the resulting rank-constrained problem into a relaxed convex optimization problem.

Notation: The transpose, the conjugate transpose (Hermitian), the Moore–Penrose inverse, the Kronecker product, and the Khatri-Rao product are denoted as $\boldsymbol{X}^{\mathrm{T}}$, $\boldsymbol{X}^{\mathrm{H}}$, $\boldsymbol{X}^{+}$, $\otimes$, $\diamond$, respectively. Moreover, diag$\{\boldsymbol{x}\}$ forms a diagonal matrix $\boldsymbol{X}$ by putting the entries of the input vector $\boldsymbol{x}$ in its main diagonal, vec$\{\boldsymbol{X}\}$ forms a vector by staking the columns of $\boldsymbol{X}$ over each other, unvec$\{\boldsymbol{x}\}$ is the inverse of the vec operator. Property 1: $\boldsymbol{x}^{\mathrm{H}}\boldsymbol{Y}\boldsymbol{x} = \mathrm{Tr}(\boldsymbol{Y}\boldsymbol{x}\boldsymbol{x}^{\mathrm{H}})$, and $\mathrm{Tr}(\boldsymbol{A}\boldsymbol{B}) = \mathrm{Tr}(\boldsymbol{B}\boldsymbol{A})$, where $\mathrm{Tr}(\cdot)$ is the trace operator.

2. System Model

In this work, an RIS-aided covert communication for the SG system as shown in figure 2, is considered, where the AMI host infrastructure in the control center of the utility company (referred to as Alice) is equipped with an antenna array with N antenna elements. Alice, which in this scenario is the base station (BS) is communicating with K smart meters (referred to as Bobs, i.e., $\mathrm{Bob}_1, \cdots, \mathrm{Bob}_K$), each equipped with a single antenna in the presence of a single antenna attacker/eavesdropper (referred to as Willie). The RIS has M passive reflecting elements uniformly arranged on a rectangular surface. The RIS has M^{h} and M^{v} elements in the horizontal and vertical directions, respectively; therefore, $M = M^{\mathrm{h}} \cdot M^{\mathrm{v}}$. A Central Processing Unit (CPU) controls Alice and the RIS via backhaul connections. According to (Wu et al., 2021), it is noted that the negligible strength of the signals reflected two or more times by the RIS was ignored due to path loss. In this work, we assume that Alice perfect knowledge of the Channel State Information (CSI) for all the channels involved. We assume perfect CSI to obtain an analytically tractable benchmark and to characterize the best achievable security enhancement performance of our proposed intelligent covert communication system under ideal channel knowledge. The extension to imperfect CSI case is left for future work.

Denote $\boldsymbol{H}_{\mathrm{ar}} \in \mathbb{C}^{M\times N}$ as the channel matrix from Alice to the RIS, $\boldsymbol{h}_{\mathrm{rb}_k} \in \mathbb{C}^{M}$ as the channel vector from the RIS to the kth Bob, and $\boldsymbol{h}_{\mathrm{ab}_k} \in \mathbb{C}^{N}$ as the channel vector from Alice to the kth Bob. Furthermore, $\boldsymbol{h}_{\mathrm{aw}} \in \mathbb{C}^{N}$ is the channel vector from Alice to Willie and $\boldsymbol{h}_{\mathrm{rw}} \in \mathbb{C}^{M}$ as the channel vector from the RIS to Willie. Therefore, for the RIS-aided covert communication system, the received signal by the kth Bob due to transmission from Alice can be expressed as

$$y_{b_k}[i] = \underbrace{\left(\boldsymbol{h}_{ab_k}^{H} + \boldsymbol{h}_{rb_k}^{H}\boldsymbol{\Theta}\boldsymbol{H}_{ar}\right)\boldsymbol{f}_{b_k}x_{b_k}[i]}_{\textit{Covert information signal}} + \underbrace{\sum_{j\neq k}\left(\boldsymbol{h}_{ab_k}^{H} + \boldsymbol{h}_{rb_k}^{H}\boldsymbol{\Theta}\boldsymbol{H}_{ar}\right)\boldsymbol{f}_{b_j}x_{b_j}[i]}_{\textit{Intra-cell interference}} + z_{b_k}[i], \qquad (1)$$

where $i \in \{1, \cdots, I\}$ denotes the number of channel use, and I is the total number of channel of uses, $\boldsymbol{\Theta} = \mathrm{diag}(\boldsymbol{\theta})$ is the RIS reflection diagonal matrix, $\boldsymbol{\theta} = [\zeta_1 e^{j\phi_1}, \cdots, \zeta_M e^{j\phi_M}]^{\mathrm{T}} \in \mathbb{C}^{M}$, where $\zeta_m \in [0,1]$ and $\phi_m \in [0,2\pi]$ denote the amplitude and phase shift associated with the mth element of the RIS, respectively. we assume that $\zeta_m = 1, \forall m$ in this work to maximize the signal reflection (Wu & Zhang, 2020). Equally, $\boldsymbol{f}_{\mathrm{b}_k} \in \mathbb{C}^{N}$ is the transmit beamforming vector with $\| \boldsymbol{f}_{\mathrm{b}_k} \|_2^2 = P_{\mathrm{b}_k}$ used by Alice to transmit the data, x_{b_k} is the zero mean covert information signal such that $\mathbb{E}\{|x_{\mathrm{b}_k}|^2\} = 1$, $z_{\mathrm{b}_k}[i]$ is Addictive White Gaussian Noise (AWGN) with variance $\sigma_{\mathrm{b}_k}^2$.

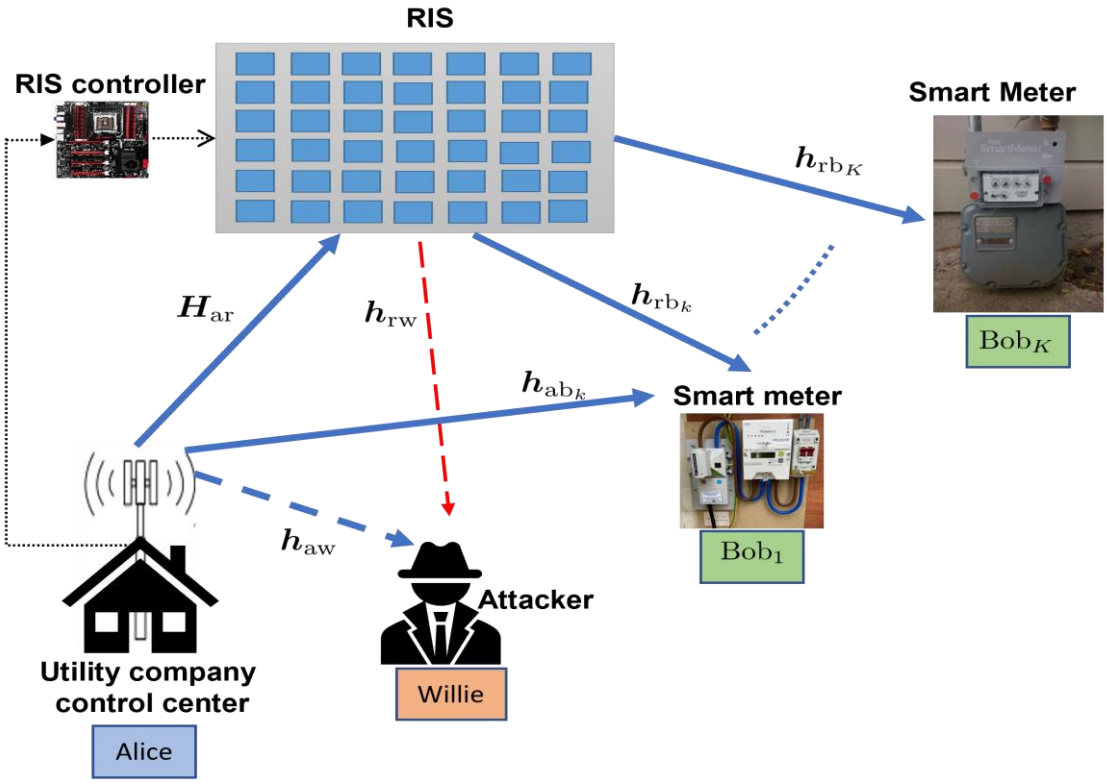


Figure 1: An RIS-aided covert communication for SG system.

Willie will perform a binary statistical hypothesis test to determine whether there is any transmission from Alice. Willie needs to distinguish between the null hypothesis, $\mathcal{H}_0$, which indicates that there is no transmission by Alice, and the alternative hypothesis, $\mathcal{H}_1$, which signifies that Alice is on for transmission. Hence, using these hypotheses, the signal received at Willie $y_w[i]$ for the ith channel is expressed as follows:

$$\begin{aligned}\mathcal{H}_0 &: y_w[i] = z_w[i] \\ \mathcal{H}_1 &: y_w[i] = \underbrace{\boldsymbol{h}_{aw}^H \boldsymbol{f}_{b_k} x_{b_k}[i]}_{Alice \rightarrow Willie} + \underbrace{\boldsymbol{h}_{rw}^H \boldsymbol{\Theta} \boldsymbol{H}_{ar} \boldsymbol{f}_{b_k} x_{b_k}[i]}_{Alice \rightarrow RIS \rightarrow Willie} + z_w[i], \end{aligned} \quad (2)$$

where $z_w[i]$ is the AWGN at Willie with zero mean and noise variance σ_w^2. Denote α_0 and α_1 as the *priori* probabilities of the hypotheses $\mathcal{H}_0$ and $\mathcal{H}_1$, respectively, where $\alpha_1 = 1 - \alpha_0$. Therefore, the total error detection for Willie's optimal test is given as

$$\beta = \alpha_0 Pr\{\mathcal{D}_1|\mathcal{H}_0\} + \alpha_1 Pr\{\mathcal{D}_0|\mathcal{H}_1\}, \quad 0 \leq \beta \leq 1 \quad (3)$$

From the above detection error rate, when $\beta = 0$, then, Willie can detect perfectly the signal transmitted by Alice. However, if $\beta = 1$, Willie can only make a blind guess. We adopt the assumption of equal *a priori* probabilities (i.e., $\alpha_0 = \alpha_1 = 0.5$), which is widely used in covert communications (Wang et al., 2020), which implies that there is a 50% chance that a transmission occurs. The primary objective for Willie in covert communication is to minimize the total detection error probability β in detecting the presence of the transmission from Alice. According to (Hu, et al., 2019), the optimal test that minimizes Willie's detection error rate is the likelihood ratio test obtained using the Neyman-Pearson criterion as (Hu, et al., 2019)

$$\frac{\mathbb{P}_1}{\mathbb{P}_0} \underset{\mathcal{D}_0}{\overset{\mathcal{D}_1}{\gtrless}} 1; \quad (4)$$

where $\mathcal{D}_0$ is the binary decision variable that indicates Alice is silent (not transmitting), and $\mathcal{D}_1$ is the binary decision variable that indicates a transmission occurred. Furthermore, $\mathbb{P}_0$ and $\mathbb{P}_1$ are the likelihood functions of Willie's observation vector over I independent use of the channel, i.e., $\boldsymbol{y}_w = \{y_w[1], \cdots, y_w[I]\}$, under $\mathcal{H}_0$ and $\mathcal{H}_1$, respectively, given as $\mathbb{P}_0 = \prod_{i=1}^{I} f\,(y_w[i]|\mathcal{H}_0)$ and $\mathbb{P}_1 = \prod_{i=1}^{I} f\,(y_w[i]|\mathcal{H}_1)$, where $f(a|b)$ is the conditional probability of event a occurring given that event b has already occurred. Therefore, from (2), the likelihood function of $y_w[i]$ under $\mathcal{H}_0$ and $\mathcal{H}_1$, is given as

$$f(y_w[i]|\mathcal{H}_0) = \mathcal{CN}(0, \sigma_w^2)$$
$$f(y_w[i]|\mathcal{H}_1) = \mathcal{CN}\left(0, |\boldsymbol{h}_{aw}^H \boldsymbol{f}_{b_k} + \boldsymbol{h}_{rw}^H \boldsymbol{\Theta} \boldsymbol{H}_{ar} \boldsymbol{f}_{b_k}|^2 + \sigma_w^2\right) \quad (5)$$

We note that based on (4), Willie's threshold for optimal detection as well as the corresponding minimum detection error rate $\hat{\beta}$, can be derived. However, due to the structure of the likelihood function in (5), the resulting equation for $\hat{\beta}$ will contain incomplete gamma functions, which makes it intractable for further analysis and design. Nonetheless, according to (Bash et al., 2015), a lower bound on $\hat{\beta}$ is used to overcome this problem of intractability; the lower bound is given as

$$\hat{\beta} \geq 1 - \sqrt{\frac{1}{2}\mathcal{D}(\mathbb{P}_0|\mathbb{P}_1)}, \quad (6)$$

where $\mathcal{D}(\mathbb{P}_0|\mathbb{P}_1)$ is the Kullback-Leibler (KL) divergence from $\mathbb{P}_0$ to $\mathbb{P}_1$, which is given as (Yan et al., 2019)

$$\mathcal{D}(\mathbb{P}_0|\mathbb{P}_1) = I\left(ln\frac{\lambda_1}{\lambda_0} + \frac{\lambda_1}{\lambda_0} - 1\right) \quad (7)$$

where $\lambda_1 = |(\boldsymbol{h}_{\mathrm{aw}}^{\mathrm{H}} + \boldsymbol{h}_{\mathrm{rw}}^{\mathrm{H}} \boldsymbol{\Theta} \boldsymbol{H}_{\mathrm{ar}}) \boldsymbol{f}_{\mathrm{b}_k}|^2$ and $\lambda_0 = \sigma_w^2$.

Generally, $\hat{\beta} \geq 1 - \xi$ is adopted as a covertness constraint, where ξ is a small value used to determine the level of the required covertness. With regards to (6), this work adopted $\mathcal{D}(\mathbb{P}_0|\mathbb{P}_1) \leq 2\xi^2$ as the covertness constraint in this work, which is a more stringent covertness constraint than $\hat{\beta} \geq 1 - \xi$ in order to achieve the desired level of covertness in the system.

3.0 Problem Formulation

The main goal of the current work is to jointly design the transmit beamforming vector $\boldsymbol{f}$ of Alice and the RIS phase shift matrix $\boldsymbol{\Theta}$ with the aim to maximize the covert rate from Alice to Bob, while taking into consideration the covertness constraint and the transmit power constraint $\| \boldsymbol{f}_{\mathrm{b}_k} \|_2^2 = P_{\mathrm{b}_k}$, $\forall k \in K$. Therefore, the resulting optimization problem can be formulated as

$$\begin{aligned} \max_{\boldsymbol{f}_{b_k}, \forall k \in K, \boldsymbol{\theta}} \quad & R_{b_k} \\ s.t. \quad & \left\|\boldsymbol{f}_{b_k}\right\|_2^2 \leq P_{b_k}, \ \forall k \in K \\ & |[\boldsymbol{\theta}]_{[m]}|^2 = 1, \ m = 1, \cdots, M \\ & \mathcal{D}(\mathbb{P}_0|\mathbb{P}_1) \leq 2\xi^2, \end{aligned} \quad (8)$$

where $R_{\mathrm{b}_k} = \log_2\left(1 + \frac{|\left(\boldsymbol{h}_{\mathrm{ab}_k}^{\mathrm{H}} + \boldsymbol{h}_{\mathrm{rb}_k}^{\mathrm{H}} \boldsymbol{\Theta} \boldsymbol{H}_{\mathrm{ar}}\right) \boldsymbol{f}_{\mathrm{b}_k}|^2}{\sum_{j \neq k} |\left(\boldsymbol{h}_{\mathrm{ab}_k}^{\mathrm{H}} + \boldsymbol{h}_{\mathrm{rb}_k}^{\mathrm{H}} \boldsymbol{\Theta} \boldsymbol{H}_{\mathrm{ar}}\right) \boldsymbol{f}_{\mathrm{b}_j}|^2 + \sigma_{\mathrm{b}_k}^2}\right)$. The first constraint in (8) is Alice's transmit power constraint, the second one is the Constant Modulus Constraints (CMCs) for the RIS reflection coefficients, and the next one is the covertness constraint. The optimization problem given in (8) is non-convex due to the non-concave objective function, joint optimization of the optimization variables $(\boldsymbol{f}_{\mathrm{ab}_k}, \boldsymbol{\theta})$, non-convex covertness constraint in the covertness constraints, and the CMCs. In the following, we adopt the AO approach to decouple the problem and exploit convex approximation techniques to reformulate and solve problem (8), obtaining a low-complexity, suboptimal solution that maximizes the covert for the various Bobs. Particularly, the main idea of the AO approach is to fix the transmit beamforming vector $\boldsymbol{f}$, and solve the resulting problem for the design of the RIS phase shifts. Then, with a fixed $\boldsymbol{\theta}$, the transmit beamforming solution is designed. The above procedure is repeated until the solution has converged, which indicates that at least a locally optimal solution to problem (8) is attained.

1.1. 3.1. Transmit Beamforming Design

The sub-problem for the design of the transmit beamforming vectors $\boldsymbol{f}_{\mathrm{b}_k}, \forall k \in K$ for a given $\boldsymbol{\theta}$ can be recast into an epigraph form by introducing an auxiliary variable ϱ_{b_k} that presented the covert rate constraint as

$$\begin{aligned} \max_{\boldsymbol{f}_{b_k}, \forall k \in K} \quad & \varrho_{b_k} \\ s.t. \quad & \frac{|\bar{\boldsymbol{h}}_{a_k}^H \boldsymbol{f}_{b_k}|^2}{\sum_{j \neq k} |\bar{\boldsymbol{h}}_{a_k}^H \boldsymbol{f}_{b_j}|^2 + \sigma_{b_k}^2} \geq \varrho_{b_k}, \\ & \left\|\boldsymbol{f}_{b_k}\right\|_2^2 \leq P_{b_k}, \ \forall k \in K \\ & ln\left(1 + \frac{|\bar{\boldsymbol{h}}_w^H \boldsymbol{f}_{b_k}|^2}{\sigma_w^2}\right) - \frac{|\bar{\boldsymbol{h}}_w^H \boldsymbol{f}_{b_k}|^2}{|\bar{\boldsymbol{h}}_w^H \boldsymbol{f}_{b_k}|^2 + \sigma_w^2} \leq \frac{2\xi^2}{I}, \end{aligned} \quad (9)$$

where we have defined $\bar{\boldsymbol{h}}_{\mathrm{a}_k}^{\mathrm{H}} = \boldsymbol{h}_{\mathrm{ab}_k}^{\mathrm{H}} + \boldsymbol{h}_{\mathrm{rb}_k}^{\mathrm{H}}\boldsymbol{\Theta}\boldsymbol{H}_{\mathrm{ar}}$ as the composite RIS-assisted channel for the kth Bob, i.e.; Alice-RIS-Bob$_k$ channel and $\bar{\boldsymbol{h}}_{\mathrm{w}}^{\mathrm{H}} = \boldsymbol{h}_{\mathrm{aw}}^{\mathrm{H}} + \boldsymbol{h}_{\mathrm{rw}}^{\mathrm{H}}\boldsymbol{\Theta}\boldsymbol{H}_{\mathrm{ar}}$ as the composite channel from Alice to Willie. Furthermore, let $\boldsymbol{F}_{\mathrm{b}_k} = \boldsymbol{f}_{\mathrm{b}_k}\boldsymbol{f}_{\mathrm{b}_k}^{\mathrm{H}}$, where $\boldsymbol{F}_{\mathrm{b}_k} \in \mathbb{C}^{N\times N}$ is a rank-one Hermitian matrix, and using Property 1, then (9) can be written as a Semidefinite Programming (SDP) problem given as

$$\begin{aligned}
\max_{\boldsymbol{F}_{b_k}, \forall k\in K} \quad & \varrho_{b_k} \\
s.t. \quad & Tr\left(\bar{\boldsymbol{H}}_{a_k}\boldsymbol{F}_{b_k}\right) \geq \varrho_{b_k}\left(\sum_{j\neq k} Tr\left(\bar{\boldsymbol{H}}_{a_k}\boldsymbol{F}_{b_j}\right) + \sigma_{b_k}^2\right), \\
& Tr\left(\boldsymbol{F}_{b_k}\right) \leq P_{b_k}, \ \forall k \in K \\
& ln\left(1 + \frac{Tr\left(\bar{\boldsymbol{H}}_w\boldsymbol{F}_{b_k}\right)}{\sigma_w^2}\right) - \frac{Tr\left(\bar{\boldsymbol{H}}_w\boldsymbol{F}_{b_k}\right)}{Tr\left(\bar{\boldsymbol{H}}_w\boldsymbol{F}_{b_k}\right)+\sigma_w^2} \leq \frac{2\xi^2}{I}, \\
& \boldsymbol{F}_{b_k} \succcurlyeq \boldsymbol{0} \\
& rank(\boldsymbol{F}_{b_k}) = 1,
\end{aligned} \tag{10}$$

where the positive semidefinite constraint in the fourth constraint in (10) and the rank-one constraint ensured that $\boldsymbol{F}_{\mathrm{b}_k} = \boldsymbol{f}_{\mathrm{b}_k}\boldsymbol{f}_{\mathrm{b}_k}^{\mathrm{H}}$ would hold after optimization. Moreover, the objective function of the optimization problem in (10) and the covertness constraint are linear functions. Additionally, the positive semidefinite constraint in the fourth constraint in (10) is a Linear Matrix Inequality (LMI), which is convex with respect to $\boldsymbol{F}_{\mathrm{b}_k}$. Furthermore, the covertness constraint in (10) can be rearranged as

$$\left(1 + \frac{\mathrm{Tr}\left(\bar{\boldsymbol{H}}_{\mathrm{w}}\boldsymbol{F}_{\mathrm{b}_k}\right)}{\sigma_w^2}\right)\ln\left(1 + \frac{\mathrm{Tr}\left(\bar{\boldsymbol{H}}_{\mathrm{w}}\boldsymbol{F}_{\mathrm{b}_k}\right)}{\sigma_w^2}\right) - \left(1 + \frac{2\xi^2}{I}\right)\frac{\mathrm{Tr}\left(\bar{\boldsymbol{H}}_{\mathrm{w}}\boldsymbol{F}_{\mathrm{b}_k}\right)}{\sigma_w^2} \leq \frac{2\xi^2}{I},$$

which is a convex constraint in terms of $\boldsymbol{F}_{\mathrm{b}_k}$. However, the optimization problem in (10) is a rank-constrained sdp problem, which is non-convex due to the rank-one constraint. This work adopts the Semi-Definite Relaxation (SDR) technique and converts the problem into a convex SDP problem by relaxing the rank-one constraint. The resulting convex SDP is expressed in (11) and can be efficiently solved using an interior point method in CVX (Grant & Boyd, 2018), for a fixed ϱ_{b_k} which can be obtained using the bisection method,

$$\begin{aligned}
\max_{\boldsymbol{F}_{b_k}, \forall k\in K} \quad & \varrho_{b_k} \\
s.t. \quad & Tr\left(\bar{\boldsymbol{H}}_{a_k}\boldsymbol{F}_{b_k}\right) \geq \varrho_{b_k}\left(\sum_{j\neq k} Tr\left(\bar{\boldsymbol{H}}_{a_k}\boldsymbol{F}_{b_j}\right) + \sigma_{b_k}^2\right), \\
& Tr\left(\boldsymbol{F}_{b_k}\right) \leq P_{b_k}, \ \forall k \in K \\
& \left(1 + \frac{Tr\left(\bar{\boldsymbol{H}}_w\boldsymbol{F}_{b_k}\right)}{\sigma_w^2}\right) ln\left(1 + \frac{Tr\left(\bar{\boldsymbol{H}}_w\boldsymbol{F}_{b_k}\right)}{\sigma_w^2}\right) - \left(1 + \frac{2\xi^2}{I}\right)\frac{Tr\left(\bar{\boldsymbol{H}}_w\boldsymbol{F}_{b_k}\right)}{\sigma_w^2} \leq \frac{2\xi^2}{I} \\
& \boldsymbol{F}_{b_k} \succcurlyeq \boldsymbol{0}
\end{aligned} \tag{11}$$

Unfortunately, due to the rank-one relaxation, the global optimal solution $\hat{\boldsymbol{F}}_{\mathrm{b}_k}$ obtained from (11) may not be a feasible solution for the original problem in (9). However, if the obtained solution is not rank-one, then the vector $\hat{\boldsymbol{f}}_{\mathrm{b}_k}$ that is feasible for the original problem is somehow extracted from the solution of the SDP problem using Gaussian randomization (Nwalozie & Haardt, 2023c).

1.2. 3.2 RIS Phase Shifts Optimization

With the designed transmit beamforming vectors $\hat{\boldsymbol{f}}_{\mathrm{b}_k}$, $\forall k \in K$, the next sub-problem is the optimization of the RIS reflection coefficients. The resulting problem for the optimization of RIS phase shifts is given as

$$\begin{aligned}
\max_{\boldsymbol{\theta},\, \varrho_{b_k}} \quad & \varrho_{b_k} \\
s.t. \quad & \frac{\left|\left(\boldsymbol{h}_{ab_k}^H + \boldsymbol{h}_{rb_k}^H\boldsymbol{\Theta}\boldsymbol{H}_{ar}\right)\boldsymbol{f}_{b_k}\right|^2}{\sum_{j\neq k}\left|\left(\boldsymbol{h}_{ab_k}^H + \boldsymbol{h}_{rb_k}^H\boldsymbol{\Theta}\boldsymbol{H}_{ar}\right)\boldsymbol{f}_{b_j}\right|^2 + \sigma_{b_k}^2} \geq \varrho_{b_k}, \\
& \left|[\boldsymbol{\theta}]_{[m]}\right|^2 = 1, \ m = 1, \cdots, M \\
& \mathcal{D}(\mathbb{P}_0|\mathbb{P}_1) \leq 2\xi^2.
\end{aligned} \tag{12}$$

For ease of simplification, let $\boldsymbol{h}_{\mathrm{aw}}^{\mathrm{H}}\boldsymbol{f}_{\mathrm{b}_k} = u_{\mathrm{aw}_k}$ and $q_{\mathrm{ab}_k} = \boldsymbol{h}_{\mathrm{ab}_k}^{\mathrm{H}}\boldsymbol{f}_{\mathrm{b}_k}$. Then, by applying the change of variables, we can write $\boldsymbol{h}_{\mathrm{rw}}^{\mathrm{H}}\boldsymbol{\Theta}\boldsymbol{H}_{\mathrm{ar}}\boldsymbol{f}_{\mathrm{b}_k} = \boldsymbol{\theta}^{\mathrm{H}}\boldsymbol{a}_{\mathrm{rw}_k}$, where $\boldsymbol{\theta} = [e^{jv_1}, \cdots, e^{jv_M}]^{\mathrm{H}}$ and $\boldsymbol{a}_{\mathrm{rw}_k} = \mathrm{diag}\{\boldsymbol{h}_{\mathrm{rw}}^{\mathrm{H}}\}\boldsymbol{H}_{\mathrm{ar}}\boldsymbol{f}_{\mathrm{b}_k}$. Similarly, the received covert information signal at the kth Bob can be written as $\left(\boldsymbol{h}_{\mathrm{ab}_k}^{\mathrm{H}} + \boldsymbol{h}_{\mathrm{rb}_k}^{\mathrm{H}}\boldsymbol{\Theta}\boldsymbol{H}_{\mathrm{ar}}\right)\boldsymbol{f}_{\mathrm{b}_k} = q_{\mathrm{ab}_k} + \boldsymbol{\theta}^{\mathrm{H}}\boldsymbol{d}_{\mathrm{ab}_k}$, where

$\boldsymbol{d}_{\mathrm{ab}_k} = \mathrm{diag}\{\boldsymbol{h}_{\mathrm{rb}_k}^{\mathrm{H}}\}\boldsymbol{H}_{\mathrm{ar}}\boldsymbol{f}_{\mathrm{b}_k}$. As a result, the sub-problem for the optimization of RIS phase shifts in (12) can be equivalently written as

$$\begin{aligned} \max_{\boldsymbol{\theta},\ \varrho_{b_k}} \quad & \varrho_{b_k} \\ s.t. \quad & \frac{|q_{ab_k}+\boldsymbol{\theta}^H\boldsymbol{d}_{ab_k}|^2}{|q_{ab_j}+\boldsymbol{\theta}^H\boldsymbol{d}_{ab_j}|^2+\sigma_{b_k}^2} \geq \varrho_{b_k}, \\ & |[\boldsymbol{\theta}]_{[m]}|^2 = 1,\ m = 1,\cdots,M \\ & ln\left(1+\frac{|u_{aw_k}+\boldsymbol{\theta}^H\boldsymbol{a}_{rw_k}|^2}{\sigma_w^2}\right) - \frac{|u_{aw_k}+\boldsymbol{\theta}^H\boldsymbol{a}_{rw_k}|^2}{|u_{aw_k}+\boldsymbol{\theta}^H\boldsymbol{a}_{rw_k}|^2+\sigma_w^2} \leq \frac{2\xi^2}{I}, \end{aligned} \tag{13}$$

where $q_{\mathrm{ab}_j} = \sum_{j\neq k}\boldsymbol{h}_{\mathrm{ab}_k}^{\mathrm{H}}\boldsymbol{f}_{\mathrm{b}_j}$ and $\boldsymbol{d}_{\mathrm{ab}_j} = \sum_{j\neq k}\mathrm{diag}\{\boldsymbol{h}_{\mathrm{rb}_k}^{\mathrm{H}}\}\boldsymbol{H}_{\mathrm{ar}}\boldsymbol{f}_{\mathrm{b}_j}$.

Furthermore, it could easily be verified that the received signal power and the received interference power at the kth Bob, as well as the received power at Willie in (13) can be rearranged into quadratic forms, respectively, as $\boldsymbol{u}^{\mathrm{H}}\boldsymbol{E}_{\mathrm{ab}_k}\boldsymbol{u}$, $\boldsymbol{u}^{\mathrm{H}}\boldsymbol{E}_{\mathrm{ab}_j}\boldsymbol{u}$, and $\boldsymbol{u}^{\mathrm{H}}\boldsymbol{G}_{\mathrm{rw}_k}\boldsymbol{u}$, where

$$\begin{aligned} \boldsymbol{u} &= \begin{bmatrix}\boldsymbol{\theta}\\ 1\end{bmatrix} \in \mathbb{C}^{M+1} \\ \boldsymbol{E}_{\mathrm{ab}_k} &= \begin{bmatrix}\boldsymbol{d}_{\mathrm{ab}_k}\boldsymbol{d}_{\mathrm{ab}_k}^{\mathrm{H}} & \boldsymbol{d}_{\mathrm{ab}_k}q_{\mathrm{ab}_k}^{*}\\ q_{\mathrm{ab}_k}\boldsymbol{d}_{\mathrm{ab}_k}^{\mathrm{H}} & |q_{\mathrm{ab}_k}|^2\end{bmatrix} \in \mathbb{C}^{(M+1)\times(M+1)} \\ \boldsymbol{E}_{\mathrm{ab}_j} &= \begin{bmatrix}\boldsymbol{d}_{\mathrm{ab}_j}\boldsymbol{d}_{\mathrm{ab}_j}^{\mathrm{H}} & \boldsymbol{d}_{\mathrm{ab}_j}q_{\mathrm{ab}_j}^{*}\\ q_{\mathrm{ab}_j}\boldsymbol{d}_{\mathrm{ab}_j}^{\mathrm{H}} & |q_{\mathrm{ab}_j}|^2\end{bmatrix} \in \mathbb{C}^{(M+1)\times(M+1)} \\ \boldsymbol{G}_{\mathrm{rw}_k} &= \begin{bmatrix}\boldsymbol{a}_{\mathrm{rw}_k}\boldsymbol{a}_{\mathrm{rw}_k}^{\mathrm{H}} & \boldsymbol{a}_{\mathrm{rw}_k}u_{\mathrm{aw}_k}^{*}\\ u_{\mathrm{aw}_k}\boldsymbol{a}_{\mathrm{rw}_k}^{\mathrm{H}} & |u_{\mathrm{aw}_k}|^2\end{bmatrix} \in \mathbb{C}^{(M+1)\times(M+1)} \end{aligned}$$

Similarly, the covertness constraint in (13) can be written as

$$\left(1+\frac{\mathrm{Tr}(\boldsymbol{G}_{\mathrm{rw}_k}\boldsymbol{U})}{\sigma_w^2}\right)\ln\left(1+\frac{\mathrm{Tr}(\boldsymbol{G}_{\mathrm{rw}_k}\boldsymbol{U})}{\sigma_w^2}\right) - \left(1+\frac{2\xi^2}{I}\right)\frac{\mathrm{Tr}(\boldsymbol{G}_{\mathrm{rw}_k}\boldsymbol{U})}{\sigma_w^2} \leq \frac{2\xi^2}{I},$$

which is convex with respect to $\boldsymbol{U}$, where $\boldsymbol{U} = \boldsymbol{u}\boldsymbol{u}^{\mathrm{H}} \in \mathbb{C}^{(M+1)\times(M+1)}$ is a rank-one Hermitian matrix. Similarly, we adopt the SDP and SDR techniques to recast the optimization problem in (13) into a rank-relaxed SDP problem, which is solved using an interior point method given as

$$\begin{aligned} \max_{\boldsymbol{U},\ \varrho_{b_k}} \quad & \varrho_{b_k} \\ s.t. \quad & Tr(\boldsymbol{E}_{ab_k}\boldsymbol{U}) \geq \varrho_{b_k}\left(Tr(\boldsymbol{E}_{ab_j}\boldsymbol{U}) + \sigma_{b_k}^2\right) \\ & |[\boldsymbol{U}]_{[m,m]}|^2 = 1,\ m = 1,\cdots,M+1 \\ & \left(1+\frac{Tr(\boldsymbol{G}_{rw_k}\boldsymbol{U})}{\sigma_w^2}\right) ln\left(1+\frac{Tr(\boldsymbol{G}_{rw_k}\boldsymbol{U})}{\sigma_w^2}\right) - \left(1+\frac{2\xi^2}{I}\right)\frac{Tr(\boldsymbol{G}_{rw_k}\boldsymbol{U})}{\sigma_w^2} \leq \frac{2\xi^2}{I} \\ & \boldsymbol{U} \succcurlyeq \boldsymbol{0}. \end{aligned} \tag{14}$$

Furthermore, if the obtained solution is not rank-one, then the RIS phase shift vector $\hat{\boldsymbol{u}}$ that is feasible for the original problem is somehow extracted from the solution of the SDR problem using Gaussian randomization. Next, the transmit beamforming vectors are updated using the $\boldsymbol{\theta}$ designed in the previous step. The alternating optimization process continues until the difference between the consecutive values of the cost function R_{ab_k} as defined in (8) becomes smaller than a given threshold $\epsilon > 0$.

4.0 Result and Discussion

In this section, we show simulation results to evaluate the performance of the proposed RIS-assisted covert communication for the SG system and other baseline schemes. We assume that Alice uses a ULA with $N = 4$ antennas, $\xi = 0.02$ as covertness level and $\sigma_{\mathrm{b}_1}^2 = \cdots \sigma_{\mathrm{b}_K}^2 = \sigma^2 = \sigma_{\mathrm{w}}^2 = 30$ dBm. We consider a SG system where Alice is communicating with $K = 3$ smart meters (i.e., 3 Bobs) at the customer's premises. These are electric, gas, and water meters. In our simulations, the Rician flat fading channel model is used, such that, for example, the channel between Alice and the RIS is represented as

$$\boldsymbol{H}_{ar} = \sqrt{\frac{\kappa}{\kappa+1}}\boldsymbol{H}_{ar}^{LOS} + \sqrt{\frac{1}{\kappa+1}}\boldsymbol{H}_{ar}^{NLOS}, \quad (15)$$

where $\kappa \geq 0$ denotes the Rician κ-factor and $\boldsymbol{H}_{\text{ar}}^{\text{NLOS}}$ represents the NLOS component, whose entries are independent and identically distributed (i.i.d.) and follow the complex Gaussian distribution with zero mean and unit variance. Furthermore, $\boldsymbol{H}_{\text{ar}}^{\text{LOS}}$ denotes the channel associated with the LOS component. In this work, $\boldsymbol{H}_{\text{ar}}^{\text{LOS}}$ is modeled according to the geometric channel model, where every channel is modeled as a summation of $L \ll \max\{M, N\}$ paths, each has a distinctive direction-of-departure (DoD) and/or direction-of-arrival (DoA) and a complex path gain (Ardah et al., 2021). For simplicity, in this work, the same value of $L = 4$ was used for all the channels.

The following baseline schemes are considered for the comparative evaluation of the developed intelligent covert communication for the SG system;

- **Baseline 1**: In this baseline scheme, an RIS is integrated into the system; however, the phase shifts of the RIS are not optimized (random phase shifts). The entries of the RIS reflection coefficient vector are randomly generated as $[\boldsymbol{\theta}]_{[m]} = e^{j\phi_m}, \forall m$, with $\phi_m \sim \mathcal{U}(-\pi, \pi)$,

- **Baseline 2**: This is considered as one of the traditional transmission schemes in the conventional SG system, which is the case where there is covert communication but no RIS is deployed, i.e., $[\boldsymbol{\theta}]_{[m]} = 0, \forall m$, (Covert without RIS). Here, Alice optimized the transmit beamforming vectors to maximize the covert rate with the covertness constraint.

- **Baseline 3**: The basic conventional transmission scheme in the SG system, without any form of covert communication, and RIS is also not deployed (No covert, no RIS). Basically, Alice designs the transmit beamforming vectors using the existing standard zero-forcing scheme.

We show the result of the average covert rate versus the SNR for the considered schemes in figure 3. The average covert rate for the system-wide covert communication for the SG system is given as $\bar{R} = \frac{1}{K}\sum_{\forall k=1}^{K} R_{\text{b}_k}$. The results show that the developed intelligent covert communication scheme for the SG system outperformed the other baseline schemes. This is due to the performance gains brought by the additional degrees of freedom offered by optimizing the RIS phase shifts. This shows that with the help of the RIS, Alice can achieve improved communication performance as well as achieve the desired covertness constraint. Equally, Baseline 1 has a better performance than the other baseline schemes. However, the performance benefits offered by the RIS are not fully exploited as the RIS phase shifts are not optimized. The performance of Baselines 2 and 3 (no RIS) further supported the benefits of integrating RIS into covert communication, as these schemes without RIS achieved a lower average covert rate. Furthermore, Baseline 3 (no covert, no RIS), considered as the basic transmission scheme in the current SG system, has the worst performance. This result demonstrates the importance of the developed intelligent covert communication scheme with regard to enhancing the security of the SG system and maintaining the integrity of the communication between the SG system and the smart meters at the customers' premises.

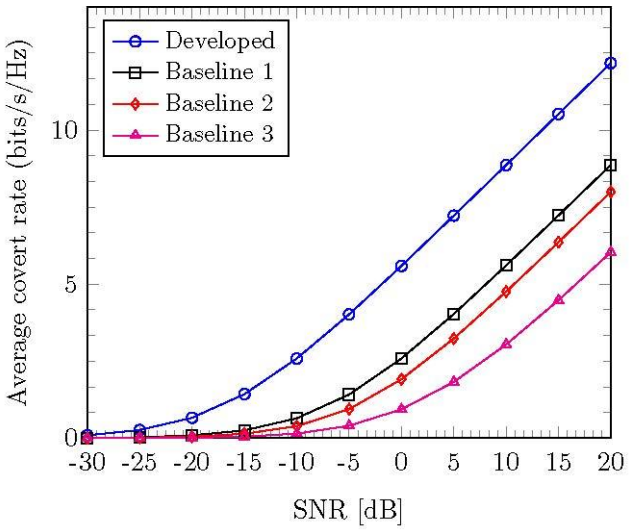


Figure 2: Average covert rate versus SNR at Alice for $M = 16, \sigma_{\text{w}}^2 = 30$ dBm, $N = 4$, $P_{\max} = 5$ dB, and $\xi = 0.02$.

In figures 4, 5, and 6 we show the performance of the developed scheme with regard to the achieved SINR versus SNR at the Electric, Water, and Gas meters, respectively. The results show that the developed scheme has a superior performance when compared with the other baseline schemes. As expected, the figures confirm that the achieved SINR increases with SNR. Since there is the availability of global CSI, the RIS phase shifts are optimized to minimize the probability of Willie detecting the transmitter's transmission behavior, thus ensuring the secure transmission of private information from Alice to the smart meters.

Moreover, in figures 8, 9 and 10 we evaluate the received signal power at Willie due to transmissions from Alice to the smart meters for the developed scheme versus SNR in comparison with other baseline schemes i.e.,

$$|\boldsymbol{h}_{\mathrm{aw}}^{\mathrm{H}}\boldsymbol{f}_{\mathrm{b}_k} + \boldsymbol{h}_{\mathrm{rw}}^{\mathrm{H}}\boldsymbol{\Theta}\boldsymbol{H}_{\mathrm{ar}}\boldsymbol{f}_{\mathrm{b}_k}|^2, \text{ where } k \in \{\text{smart meters}\}.$$

The results show that the received power at Willie for schemes with RIS is lower than that of schemes without RIS in all scenarios. These results further justify the security enhancement achieved by the integration of the RIS in the SG system. The result implied that by the optimization of the RIS phase shifts, Alice can transmit with high transmit power while simultaneously achieving improved covert communication and ensuring that the covertness constraint is satisfied, thereby deteriorating Willie's detection ability. However, we note that the performance of Baseline 1 suggests that with random phase shifts for the RIS, covertness is achieved only by the transmit beamforming vectors, and these random phase shifts of the RIS can be exploited by Willie. Therefore, we note that whereas RIS improves communication performance via the optimization of its phase shifts, it can serve as an additional source of exploits if the phase shifts are not optimized.

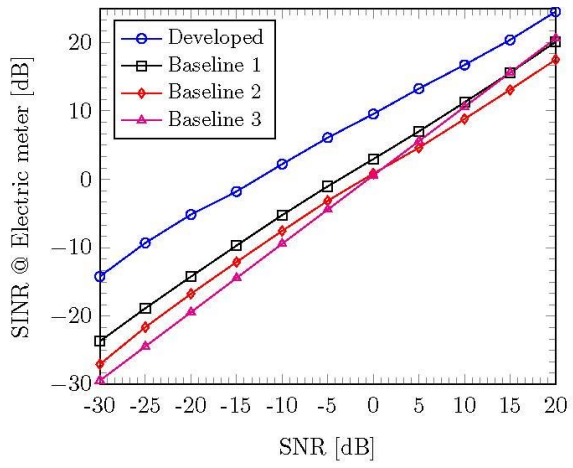


Figure 3: achieved SINR at the Electric Meter

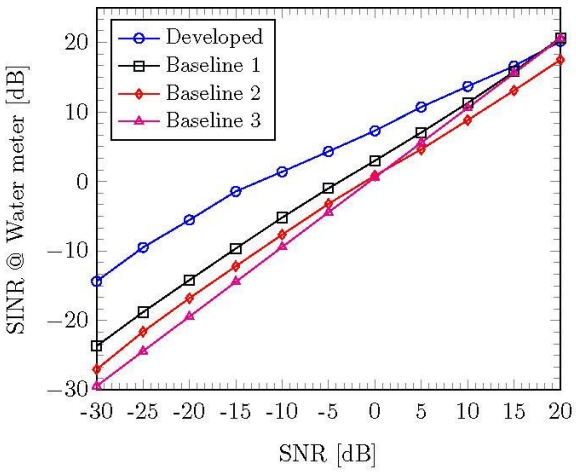


Figure 4: achieved SINR at the Water Meter

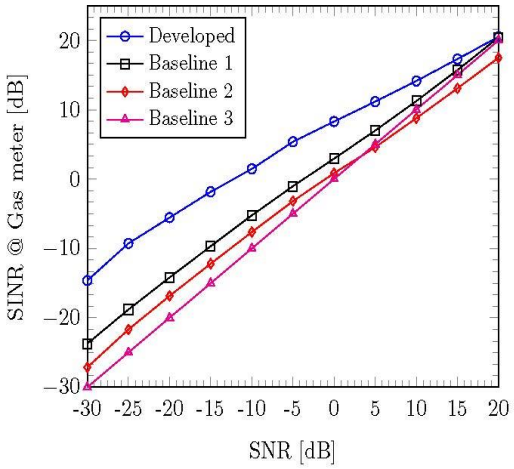


Figure 5: achieved SINR at the Gas meter with $M = 16, \sigma_{\mathrm{w}}^2 = 30$ dBm, $N = 4$, $P_{\max} = 5$ dB, and $\xi = 0.02$.

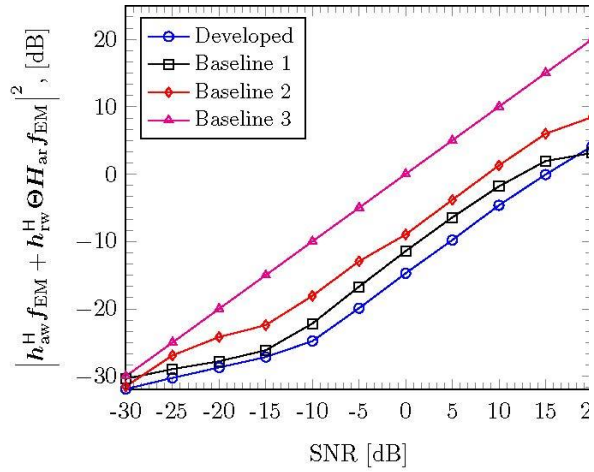


Figure 6: received power at Willie due to transmission from Alice to the Electric Meter

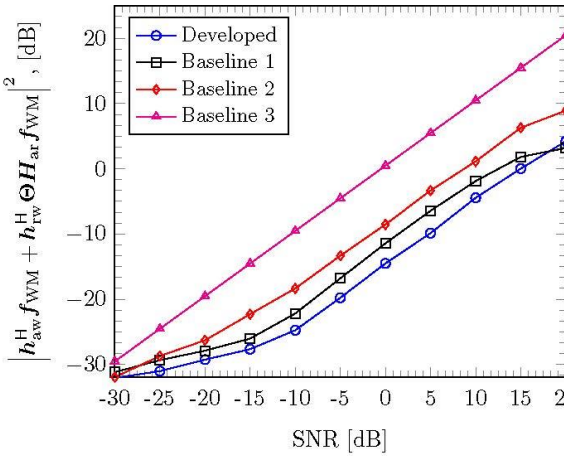


Figure 7: received power at Willie due to transmission from Alice to the Water Meter

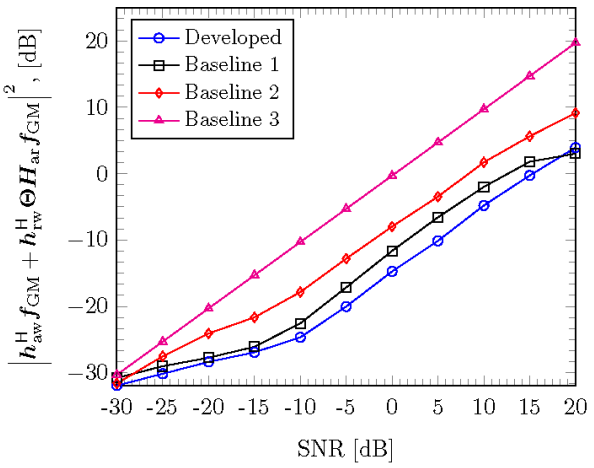


Figure 8: received power at Willie with $M = 16, \sigma_w^2 = 30$ dBm, $N = 4$, $P_{max} = 5$ dB, and $\xi = 0.02$.

Furthermore, we evaluate the false alarm probability at Willie, i.e., $\Pr\{\mathcal{D}_1|\mathcal{H}_1\}$ in figure 10, which is the probability that Willie concludes that there is a transmission from Alice, while Alice is silent. The results show that the proposed intelligent covert communication scheme performs better than the other baseline schemes. These results further justify the security enhancement achieved by the integration of the RIS in the SG system. The result implied that by optimizing RIS phase shifts, while satisfying the covertness constraint, Willie's probability of accurately concluding whether there is transmission from Alice or not has been reduced. Higher probability implies that Willie correctly concludes that Alice is silent. Additionally, in figure 11, the miss detection probability of Willie is evaluated as a function of the different transmitting power, i.e., $\Pr\{\mathcal{D}_0|\mathcal{H}_1\}$, which is the probability that Willie mistakenly decides that there is no transmission when in reality Alice is transmitting. According to the figure, the developed intelligent covert communication scheme performed better than other baseline schemes. Since a higher miss detection probability implies that Willie correctly decides that there is a transmission from Alice. Recall that from the perspective of Alice, the main objective in achieving covert communication

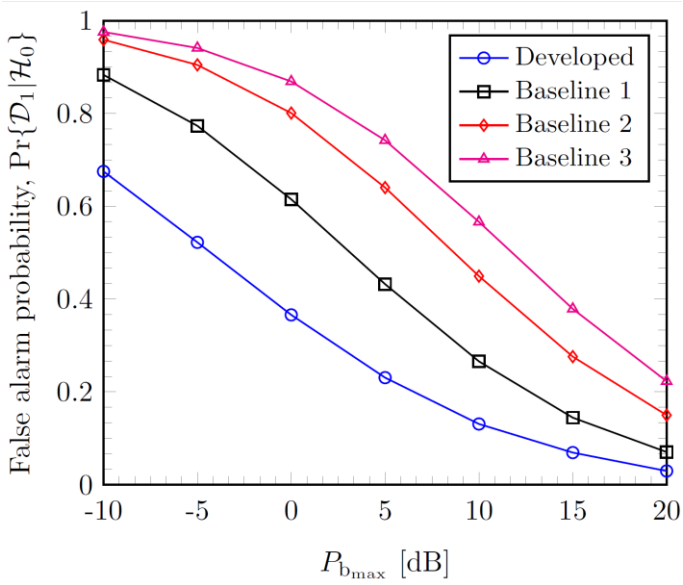


Figure 10: false alarm probability of Willie

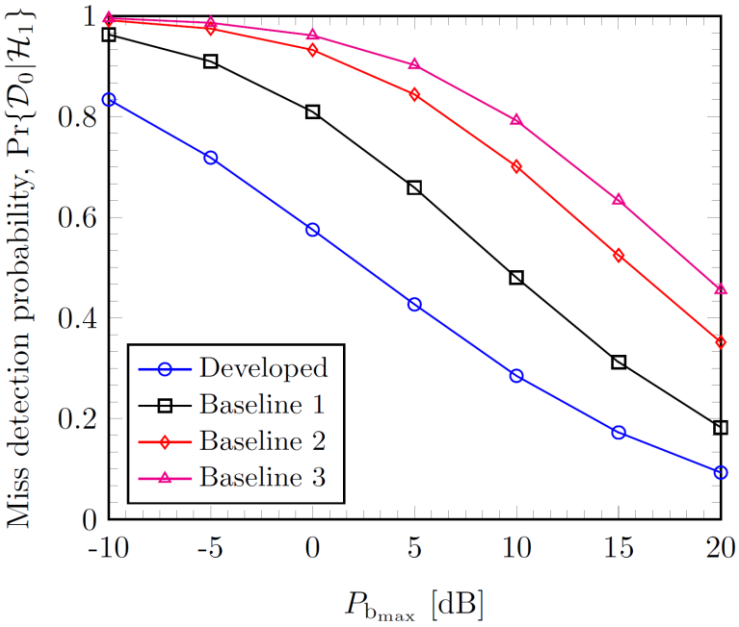


Figure 11: miss detection probability

4.0. Conclusion

We consider the joint design of the transmit beamforming and RIS reflection coefficient in an RIS-aided covert communication network to maximize the covert rate for the various smart meters (Bobs) and minimize the probability of the monitor/attacker (Willie) detecting the transmitter's transmission behaviour, thus ensuring the secure transmission of private information. To obtain a solution, we adopt the alternating optimization technique and decouple the optimization problem, as well as exploit some convex approximation techniques and reformulate the optimization problem; and obtained a low-complexity and sub-optimal solution that maximizes the covert rate at the various Bobs as well as ensures that the covertness constraint is satisfied. The security enhancement offered by the developed intelligent covert communication scheme is evaluated in comparison with other baseline schemes. The results obtained show that the developed scheme has superior performance in terms of the average cover rate than the baseline schemes. The obtained results show the performance benefits obtainable by the integration of the RIS in the SG system, as baseline schemes without RIS have the worst performance in all the evaluated scenarios.

References

Agung, A. A. G., & Handayani, R. (2022). Blockchain for smart grid. *Journal of King Saud University Computer and Information Sciences*, *34*(3), 666–675. https://doi.org/https://doi.org/10.1016/j.jksuci.2020.01.002

Ardah, K., Gherekhloo, S., de Almeida, A. L. F., & Haardt, M. (2021). TRICE: A Channel Estimation Framework for RIS-Aided Millimeter-Wave MIMO Systems. *IEEE Signal Processing Letters*, *28*, 513–517. https://doi.org/10.1109/LSP.2021.3059363

Bash, B. A., Goeckel, D., Towsley, D., & Guha, S. (2015). Hiding information in noise: Fundamental limits of covert wireless communication. *IEEE Communications Magazine*, *53*(12), 26–31. https://doi.org/10.1109/MCOM.2015.7355562

Bishowjit, P., Auvizit, S., Sarafat, H. A., Sajal, K. D., & Nazmus, S. (2024). Potential smart grid vulnerabilities to cyber-attacks: Current threats and existing mitigation strategies. *Heliyon*, *10*(19). https://doi.org/10.1016/j.heliyon.2024.e37980

Gherekhloo, S., Ardah, K., Nwalozie, G. C., Almeida, A. L. F. de, & Haardt, M. (2024). An efficient channel training protocol for channel estimation in double RIS-aided MIMO systems. *Proc. of 32nd European Signal Processing Conference (EUSIPCO 2024), Lyon, France*. https://doi.org/10.23919/EUSIPCO63174.2024.10715192

Gong, S., Lu, X., Hoang, D. T., Niyato, D., Shu, L., Kim, D. I., & Liang, Y.-C. (2020). Toward smart wireless communications via intelligent reflecting surfaces: A contemporary survey. *IEEE Communications Surveys Tutorials*, *22*(4), 2283–2314. https://doi.org/10.1109/COMST.2020.3004197

Grant, M., & Boyd, S. (2018). *CVX: MATLAB software for disciplined convex programming*. http://cvxr.com/cvx

Hu, J.; Yan, S.; Zhou, X.; Feng, S.; & Li, J (2019). Covert wireless communications with channel inversion power control in Rayleigh fading. *IEEE Trans. Veh. Technol*. 2019, 68, 12135−12149

Lieskovan, T., Hajny, J., & Cika, P. (2019). Smart Grid Security: Survey and Challenges. In *Proc. of 2019 11th International Congress on Ultra-Modern Telecommunications and Control Systems and Workshops (ICUMT)*. https://doi.org/10.1109/ICUMT48472.2019.8970738

Nwalozie, G. C., Ardah, K., & Haardt, M. (2022). Reflection Design methods for Reconfigurable Intelligent Surfaces-aided Dynamic TDD Systems. *Proc. of 12th IEEE Sensor Array and Multichannel Signal Processing Workshop (SAM 2022), Trondheim, Norway*. 2022 IEEE 12th Sensor Array and Multichannel Signal Processing Workshop (SAM). https://doi.org/10.1109/SAM53842.2022.9827850

Nwalozie, G. C., & Haardt, M. (2023a). Distributed Coordinated Beamforming for RIS-aided Dynamic TDD Systems. *Proc. of 26th International ITG Workshop on Smart Antennas and 13th Conference on Systems, Communications, and Coding (WSA and SCC 2023), Braunschweig, Germany*.

Nwalozie, G. C., & Haardt, M. (2023b). Leakage-based Coordinated Beamforming for RIS-aided Dynamic TDD Systems. *Proc. of 31st European Signal Processing Conference (EUSIPCO 2023), Helsinki, Finland*. https://doi.org/10.23919/EUSIPCO58844.2023.10289836

Nwalozie, G. C., & Haardt, M. (2023c). Robust Beamforming for RIS-aided Dynamic TDD Systems. *Proc. of 31st European Signal Processing Conference (EUSIPCO 2023), Helsinki, Finland*. https://doi.org/10.23919/EUSIPCO58844.2023.10289990

Nwalozie, G. C., & Haardt, M. (2024). Probabilistic-constrained robust Beamforming for RIS-aided Dynamic TDD Systems. *Proc. Of 19th International Symposium on Wireless Communication Systems (ISWCS 2024), Rio de Janeiro, Brazil*. https://doi.org/10.1109/ISWCS61526.2024.10639180

Onoshakpor, R. M., & Okafor, K. C. (2017). Cyber security in smart grid convolution networks (SGCNs). *2017 IEEE 3rd International Conference on Electro-Technology for National Development (NIGERCON)*, 392–399. https://doi.org/10.1109/NIGERCON.2017.8281911

Pogaku, A. C., Do, D.-T., Lee, B. M., & Nguyen, N. D. (2022). UAV-assisted RIS for future wireless communications: A survey on optimization and performance analysis. *IEEE Access*, *10*, 16320–16336. https://doi.org/10.1109/ACCESS.2022.3149054

Rohokale, V., & Prasad, R. (2016). Cyber security for smart grid - the backbone of social economy. *Journal of Cyber Security and Mobility*, *5*(1), 55–76. https://doi.org/10.13052/jcsm2245-1439.514

Upadhyay, D., & Sampalli, S. (2020). SCADA (Supervisory Control and Data Acquisition) systems: Vulnerability assessment and security recommendations. In *Computers & Security* (Vol. 89, pp. 1–18). https://doi.org/10.1016/j.cose.2019.101666

Wang, H., Zhang, Y., Zhang, X., & Li, Z. (2020). Secrecy and covert communications against UAV surveillance via multi-hop networks. *IEEE Transactions on Communications*, *68*(1), 389–401. https://doi.org/10.1109/TCOMM.2019.2950940

Wu, Q., & Zhang, R. (2020). Towards smart and reconfigurable environment: Intelligent reflecting surface aided wireless network. *IEEE Communications Magazine*, *58*(1), 106–112. https://doi.org/10.1109/MCOM.001.1900107

Wu, Q., Zhang, S., Zheng, B., You, C., & Zhang, R. (2021). Intelligent reflecting surface-aided wireless communications: A tutorial. *IEEE Transactions on Communications*, *69*(5), 3313–3351. https://doi.org/10.1109/TCOMM.2021.3051897

Yan, S., He, B., Zhou, X., Cong, Y., & Swindlehurst, A. L. (2019). Delay-intolerant covert communications with either fixed or random transmit power. *IEEE Transactions on Information Forensics and Security*, *14*(1), 129–140. https://doi.org/10.1109/TIFS.2018.2846257

Yuan, J., Liang, Y.-C., Joung, J., Feng, G., & Larsson, E. G. (2021). Intelligent reflecting surface-assisted cognitive radio system. *IEEE Transactions on Communications*, *69*(1), 675–687. https://doi.org/10.1109/TCOMM.2020.3033006